# DETC2017/MR-12345

# DESIGN OF A SPATIAL SIX-BAR FLAPPING WING MECHANISM FOR COMBINED CONTROL OF SWING AND PITCH

#### Peter L. Wang

Robotics and Automation Laboratory, University of California Irvine, California 92697 Email: wangpl1@uci.edu

# **ABSTRACT**

This paper presents a design procedure to achieve a flapping wing mechanism for a micro air vehicle that drives both the swing and pitch movement of the wing with one actuator. The mechanism combines a planar four bar linkage with a spatial RSSR attached to the input and output links forming a spatial Stephenson six-bar linkage. Function generation synthesis yields a planar four-bar that controls the wing swing profile. The pitch control is synthesized by inverting the movement of the combined system to isolate and compute the SS chain. In order to ensure the design achieves the specified task precision points, the SS chain was randomized within a prescribed tolerance zone. The result was 29 designs, one of which is presented in detail.

#### 1 Introduction

Flapping Wing Micro Air Vehicles (FWMAV) are flying crafts that are small winged aircrafts generally smaller than 15cm. The majority of FWMAV mimic insect's and rely on wings that swing in a planar path without control of wing pitch. It is adjusted passively using the drag force of the air to position the wing. See for example, the Aerovironment Nano Air Vehicle [1]. Recent research by Taha, et al [2, 3] shows that pitch control can provide improved flight aerodynamics.

This paper presents the synthesis of a flapping wing mechanism to achieve the wing swing and pitch profiles identify by Taha. The result is an RSSR connecting the input and output joints of a planar four bar linkage, which forms a spatial Steven-

## J. Michael McCarthy

Robotics and Automation Laboratory, University of California Irvine, California 92697 Email:jmmccart@uci.edu

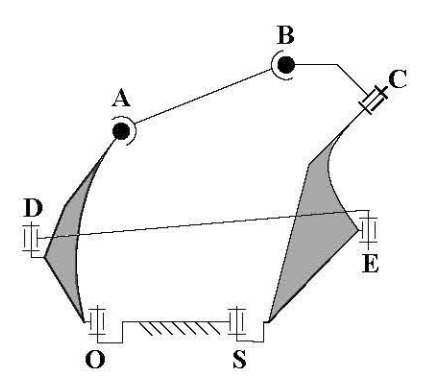


**FIGURE 1**. The diagram shows the structure of the spatial Stevenson I six bar mechanism

son I six bar mechanism, see 1.

We present the design methodology for this flapping wing mechanism and obtain a useful design.

#### 2 Literature Review

The synthesis of four-bar function generators define the dimensions of the linkage to obtain a specified relationship between the input and output joint angles, see Svoboda [4] and Freudenstein [5]. In our case this transforms a constant rotation of the input to a specified reciprocating wing swing movement.

The synthesis of the RSSR function generators is presented by Denevit and Hartenberg [6]. Suh [7] designed RSSR function

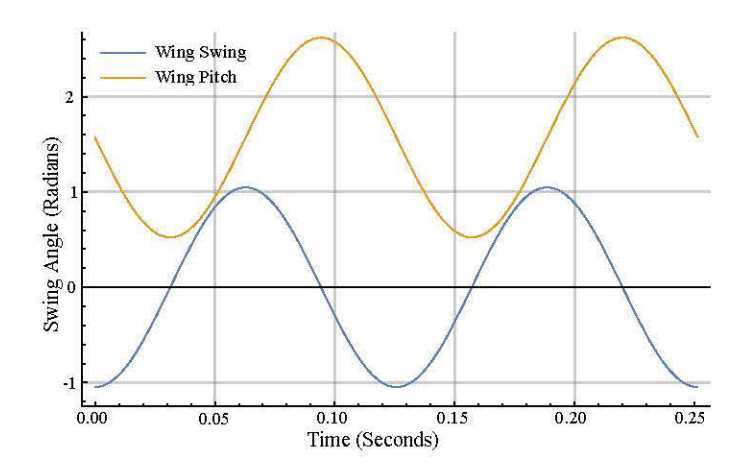


**FIGURE 2**. The wing swing and wing pitch functions.

generators by inversion of the SS constraint equation, also see Gupta [8].

The assembly of the RSSR joining the input and output cranks of the planar four-bar linkage creates a spatial Stephenson I linkage. Dinghra [9] describes the synthesis of planar six-bar linkages. Plecnik and McCarthy [10] obtained the complete solutions to Dinghra's six-bar design equations. Bai [11] generated a unified formulation for motion generation for Stephenson linkages I, II, and III. Zhao, Purwar, and Ge [12] have developed a unified method of synthesizing four and six bar planar linkages with both R and P joints using planar quaternions.

There seem to be no references to the synthesis of a spatial six-bar linkage of the form we use to provide simultaneous control of the swing and pitch of our micro air vehicle [13].

## 3 Wing Swing and Pitch Requirements

A study of flapping wing designs for micro air vehicles [13] shows that planar crank-rocker linkages with a passive position of the wing pitch provide effective wing performance. However, Yan and Taha [14] show that coordinated control of the pitch and wing movement improves the aerodynamics of a micro air vehicle.

They demonstrate effective aerodynamic performance with swing and pitch functions,  $q(\theta)$  and  $\phi(\theta)$ , given by

$$q(\theta) = \frac{\pi}{2} - \frac{\pi}{3}\cos\theta, \quad \phi(\theta) = \frac{\pi}{2} - \frac{\pi}{3}\sin\theta, \tag{1}$$

where the driving angle is  $\theta = \omega t$ , and  $\omega$  is the flapping frequency, Figure 2.

#### 4 Synthesis of the Swing Mechanism

In order to design the swing mechanism, we follow Brodell and Soni [15] to obtain a four-bar linkage that has a time ratio

of one. This ensures the speed of the flapping movement is the same in both the up and down strokes.

Brodell and Soni provide formulas for the link lengths parameterized by the desired swing angle  $\sigma$  and transmission angle  $\lambda$ .

$$\frac{r_3}{r_1} = \sqrt{\frac{1 - \cos \sigma}{2 \cos^2 \lambda}}, \quad \frac{r_4}{r_1} = \sqrt{\frac{1 - (r_3/r_1)^2}{1 - (r_3/r_1)^2 \cos^2 \lambda}}, 
\frac{r_2}{r_1} = \sqrt{\left(\frac{r_3}{r_1}\right)^2 + \left(\frac{r_4}{r_1}\right)^2 - 1},$$
(2)

where  $r_1$ ,  $r_2$ ,  $r_3$ , and  $r_4$  are the lengths of the ground link, the input crank, the coupler link, and the follower link, respectively.

Given the link lengths of the crank-rocker, the swing function  $\gamma(\Delta\theta)$  where  $\Delta\theta$  is measured from the line NG of the linkage, McCarthy [16],

$$A(\Delta\theta)\cos\gamma + B(\Delta\theta)\sin\gamma = C(\Delta\theta), \tag{3}$$

where

$$A(\Delta\theta) = 2r_2r_4\cos\Delta\theta - 2r_1r_4, \quad B(\Delta\theta) = 2r_2r_4\sin\Delta\theta, C(\Delta\theta) = r_1^2 + r_2^2 + r_4^2 - r_3^2 - 2r_1r_2\cos\Delta\theta.$$
 (4)

This has the solution,

$$\gamma(\Delta\theta) = \arctan\left(\frac{B}{A}\right) \pm \arccos\left(\frac{C}{\sqrt{A^2 + B^2}}\right).$$
(5)

Our goal is to achieve the four-bar linkage output  $\bar{\gamma}(\theta) = \gamma(\theta_0 + \Delta\theta) + k_0$  that matches the swing function  $q(\theta)$  at  $\theta = 0$  and where  $q(0) = \pi/6$  and the minimum of  $\gamma$  is at  $\gamma(0.045) = 0.568$ . Thus,  $0 = \theta_0 + 0.045$  and  $\pi/6 = 0.568 + k_0$ . The result is  $\theta_0 = -0.045$ , or -2.6 degrees and  $k_0 = 0.045$  or 2.6 degrees, as seen in Figure 3.

Thus we obtain

$$\bar{\gamma} = \gamma (\Delta \theta - 0.045) + 0.045$$
 (6)

## 5 Synthesis of the Pitch Mechanism

In order to control the pitch of the flapping wing, we introduce an RSSR linkage connecting the input and output links of the swing mechanism that will orient the pitch of the wing during the flapping movement.

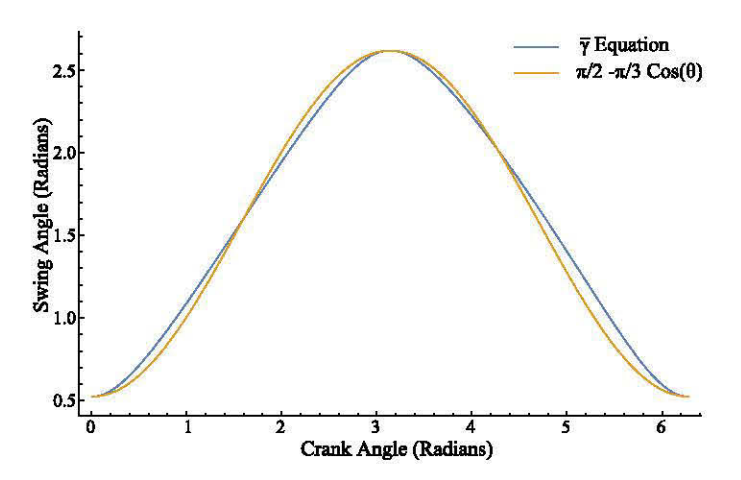


**FIGURE 3.** Comparison of the task swing function  $q(\theta)$  and the output of the swing mechanism  $\bar{\gamma}(\theta)$ .

The swing mechanism **NDEG** is shown in Figure 4 positioned in the ground frame G so that the fixed pivot of the output crank **GE** is at the origin and the axes of the four joints are directed along the x-axis of G. This output crank swing back and forth providing the flapping movement, which causes the axis **CS** of the wing to swing back and forth. The dimension  $g = |\mathbf{GS}|$  is selected by the designer. The output crank **CB** of the RSSR linkage controls the pitch of the wing around the axis **CS**.

The location of the fixed pivot N = (0, t, d) of input crank ND is selected by the designer so that the ground link GN has the length  $r_1$ . The input ND of the swing mechanism also drives the input OA to the RSSR pitch mechanism around the axis NO.

Our goal is to determine these dimensions by solving the SS constraint equations for seven values of the pitch function,  $\phi_i = \phi(\theta_i)$ , i = 1, ..., 7, see [16]. The values  $\phi(\theta_i)$ , which are chosen using Chebyshev spacing along the pitch function [17].

The synthesis equations coordinate the rotation of the link **OA**, **CS** and **BC** links so that they simultaneously satisfy,  $\bar{\gamma}_i = \bar{\gamma}(\theta_i)$  and  $\phi_i = \phi(\theta_i), i = 1, \dots, 7$ .

The homogeneous transforms  $\mathbf{Z}$  and  $\mathbf{X}$  that define coordinate screw displacement about the x and z axes, given by,

$$\mathbf{Z}(\theta, d) = \begin{bmatrix} \cos \theta - \sin \theta & 0 & 0 \\ \sin \theta & \cos \theta & 0 & 0 \\ 0 & 0 & 1 & d \\ 0 & 0 & 0 & 1 \end{bmatrix}, \mathbf{X}(\alpha, a) = \begin{bmatrix} 1 & 0 & 0 & a \\ 0 & \cos \alpha - \sin \alpha & 0 \\ 0 & \sin \alpha & \cos \alpha & 0 \\ 0 & 0 & 0 & 1 \end{bmatrix}$$
(7)

are used to locate the axis of rotation **NO** for the input to the RSSR linkage and the axis **CS** of its output, Figure 4.

The rotation axis NO of the input crank is defined by the

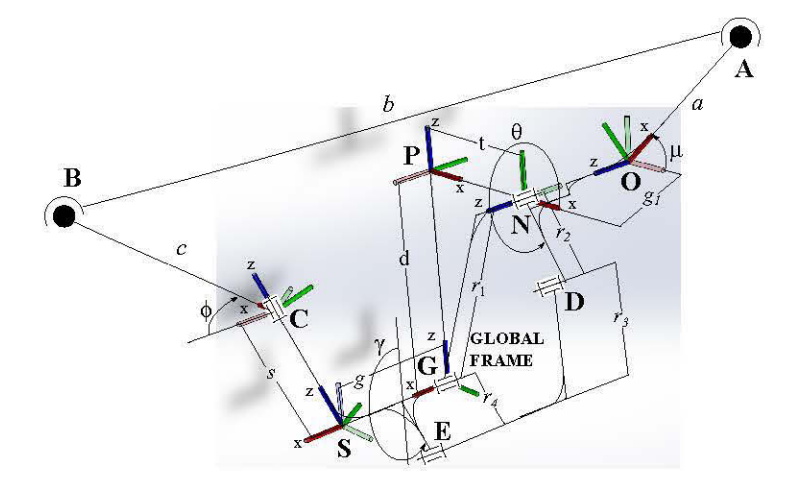


**FIGURE 4**. The diagram shows the RSSR and Planar Four Bar mechanism and the frames of reference used to define the rotation axes.

sequence of transformations,

$$\mathbf{H}(\boldsymbol{\theta}) = \mathbf{Z}(\pi/2, d)\mathbf{X}(\pi/2, t)\mathbf{Z}(\boldsymbol{\theta}, 0), \tag{8}$$

where the parameter  $\theta$  defines the rotation of the link **NOA** and  $(\pi/2,d)$  and  $(\pi/2,t)$  define its position relative to the ground frame, see Figure 4. Let  $\mathbf{H}_{i1}$  be the transformation relative to the initial configuration of the RSSR chain evaluated at seven task angles  $\theta_i$ ,  $i=1,\ldots,7$ , so we have,

$$\mathbf{H}_{i1} = \mathbf{H}_i \mathbf{H}_1^{-1}, \quad i = 1, \dots, 7.$$
 (9)

The rotation axis SC of the output crank is defined by the sequence of transformations,

$$\mathbf{J}(\phi, \bar{\gamma}) = \mathbf{X}(\bar{\gamma}, g)\mathbf{Z}(\phi, 0), \tag{10}$$

where  $(\bar{\gamma}, g)$  defines the position relative to the ground frame, and  $\phi$  defines the rotation of the output crank. Let  $J_{i1}$  denote the transformation relative to the initial configuration of the RSSR chain evaluated at seven task angles  $\phi_i$ , i = 1, ..., 7,

$$\mathbf{J}_{i1} = \mathbf{J}_i \cdot \mathbf{J}_1^{-1} \quad i = 1, \dots, 7.$$
 (11)

The design equations for pitch mechanism are obtained as the constraint that the length of the SS link be constant in each of the task positions specified by  $\phi_i = \phi(\theta_i)$ ,  $i = 1, \dots, 7$ . Let the coordinates of the centers **A** and **B** of the S-joints in the first task position be given by

$$\mathbf{A}^{1} = (u, v, w), \quad \mathbf{B}^{1} = (x, y, z).$$
 (12)

Copyright © 2017 by ASME

Then the constraint that the coupler link **AB** to be of constant length  $b = |\mathbf{AB}|$  in each of the task positions yields the equations,

$$|\mathbf{A}^{i} - \mathbf{B}^{i}|^{2} = |([\mathbf{H}_{i1}]\mathbf{A}^{1} - [\mathbf{J}_{i1}]\mathbf{B}^{1})|^{2} = b^{2}, \quad i = 1, \dots, 7.$$
 (13)

These equations can be reduced to a degree 20 polynomial [18, 16], and thus the system of equations has a maximum of 20 unique solutions. This set of equations was solved using Mathematica which yielded values for the points  $\mathbf{A}^1 = (u, v, w)$  and  $\mathbf{B}^1 = (x, y, z)$ . The solutions found are all possible solutions for the set of specified dimensions and angles.

#### 6 Analysis of the Pitch Mechanism

In order to evaluate the linkage obtained from the synthesis routine, we analyze RSSR for each configuration of the swing four-bar linkage. The goal is to verify that the mechanism moves smoothly through the specified swing and pitch movements. Every solution from the synthesis is analyzed.

The constraint equation of the RSSR chain defines the length of the link **AB** in terms of  $\Delta\theta$ ,  $\bar{\gamma}$  and  $\phi$ , given by,

$$|[\mathbf{H}(\Delta \theta)]\mathbf{a} - [\mathbf{J}(\phi, \bar{\gamma})]\mathbf{b}|^2 = b^2, \tag{14}$$

where  $\mathbf{H}$  and  $\mathbf{J}$  are given in (8) and (10) and

$$\mathbf{a} = [\mathbf{H}_1]^{-1} \mathbf{A}^1 = (\bar{u}, \bar{v}, \bar{w}), \quad \mathbf{b} = [\mathbf{J}_1]^{-1} \mathbf{B}^1 = (\bar{x}, \bar{y}, \bar{z}).$$
 (15)

For each value of  $\Delta\theta$ , we obtain  $\bar{\gamma}$ , and obtain an equation of the form,

$$A(\Delta\theta)\cos\phi + B(\Delta\theta)\sin\phi = C(\Delta\theta), \tag{16}$$

where

$$A(\Delta\theta) = -2d\bar{y}\sin\gamma + 2g\bar{x} - 2t\bar{y}\cos\gamma - 2\bar{u}\bar{y}\cos(\gamma - \Delta\theta) - 2\bar{v}\bar{y}\sin(\gamma - \Delta\theta) - 2\bar{w}\bar{x}$$

$$B(\Delta\theta) = -2(d\bar{x}\sin\gamma + g\bar{y} + t\bar{x}\cos\gamma + \bar{u}\bar{x}\cos(\gamma - \Delta\theta) + \bar{v}\bar{x}\sin(\gamma - \Delta\theta) - \bar{w}\bar{y})$$

$$C(\Delta\theta) = -b^2 + d^2 + t^2 + g^2 + \bar{x}^2 + \bar{y}^2 + \bar{z}^2 + \bar{u}^2 + \bar{v}^2 + \bar{w}^2 2d\bar{u}\sin\Delta\theta + 2d\bar{v}\cos\Delta\theta - 2d\bar{z}\cos\gamma - 2g\bar{w} + 2t\bar{u}\cos\Delta\theta - 2t\bar{v}\sin\Delta\theta + 2t\bar{z}\sin\gamma + 2\bar{u}\bar{z}\sin(\gamma - \Delta\theta) - 2\bar{v}\bar{z}\cos(\gamma - \Delta\theta)$$

$$(17)$$

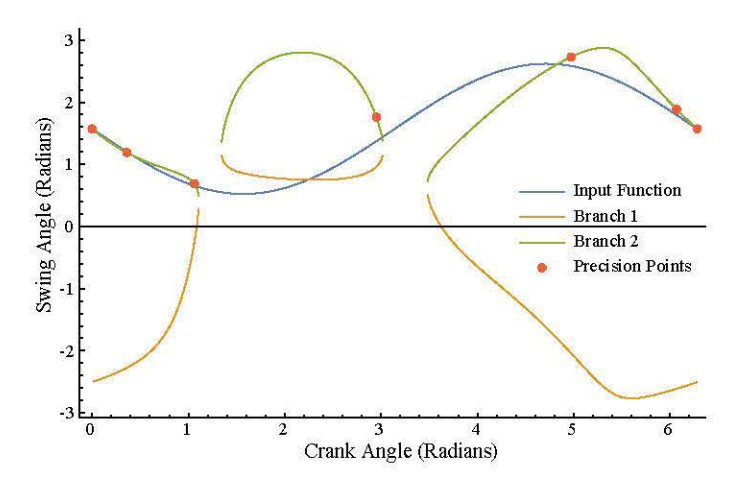


**FIGURE 5**. The plot of a non-continuous solution.

where g, t and d are determined by the designer.

Solve for  $\phi_i(\Delta \theta_i)$  i = 1,...,7 using Eq 5.

The solutions that pass through all precision points on a single branch pass the branching analysis. The passing solutions are then checked for continuity. The range of the input crank angles is divided into two hundred intermediate angles and the links are checked to ensure that they do not change length at the intermediary positions. The solutions are plotted for the entire range of motion of the input crank. An example of a solution that fails in continuity, but passes branching is shown in Figure 5.

For the physical construction of the linkage, shifts need to be introduced from the input and output links as seen previously in the planar linkage. The goal is for  $\bar{\phi}_i + \phi_s = \phi_i(\mu_i) = \phi_i(\Delta\theta_i + \theta_s)$  for  $i=1,\ldots,7$ , where  $\mu_1$  is the angle of  $\mathbf{A}^1$  and the x-axis of Frame O about line  $\mathbf{NO}$  and  $\rho_1$  is the angle between  $\mathbf{B}^1$  and the x-axis of Frame C about the line  $\mathbf{CS}$ . This results in  $\bar{\phi} = \phi_i(\Delta\theta + \theta_s) - \phi_s \ \phi_s = \rho_1 - \phi_1$  and  $\theta_s = \mu_1 - \Delta\theta_1$ .

#### 7 Design Methodology

Our design methodology consists of threes steps: i) the required swing movement is used to design a planar four-bar function generator;, ii) the coordinate pitch movement is used to formulate and solve the SS chain constraints for inverted task positions within specified tolerance zones, and iii) each solution is analyzed to evaluate its continuous movement through the task positions. This process is iterated with randomly selected task positions within the tolerance zones. Successful design candidates are collected, ranked and evaluated by the designer.

## 8 Example Flapping Wing Mechanism

The precision points of  $\theta$  and  $\phi$  were chosen by applying Chebyshev Spacing on Equation 1. The calculated input crank angles( $\theta$ ) are then substituted into the planar linkage equation,

see Eq 6, to obtain the wing swing angle  $\bar{\gamma}$ . The values are seen in Table 1.

	Pitch Angle Requirements (Radians)									
i	1	2	2 3 4 5 6							
$\theta_i$	0	0.153	1.295	3.141	4.988	6.129	6.283			
$\delta  heta_i$	0		±0.262							
$\phi_i$	1.570	1.410	0.563	1.570	2.578	1.731	1.571			
$\delta\phi_i$	0		0							
$ar{\gamma}_i$	0.524	0.545	1.339	2.618	1.413	0.546	0.524			

**TABLE 1**. Table of initial parameter angles for seven precision points.

The planar mechanism was chosen to have a total swing angle  $\sigma = \pi/3$  from  $q(\theta)$  in Eq 5, a base length  $r_1 = 5$ , and a transmission angle of 0.521 or 29.9 degrees. The corresponding values of  $r_2$ ,  $r_3$ , and  $r_4$  are seen in Table 2. These values are substituted into Eq 5 which gives  $\gamma(\theta)$  a minimum at  $\gamma(0.045) = 0.568$ . Thus,  $\theta_0 = -0.045$  or -2.6 degrees and  $k_0 = 0.045$  or 2.6 degrees and the swing equation is

$$\bar{\gamma}(\Delta\theta) = \tan^{-1} \frac{2.24 - 0.17\cos(\Delta\theta + 0.04)}{-0.17\sin(\Delta\theta + 0.04)} + \cos^{-1} \left( \frac{4.33\cos(\Delta\theta + 0.04) - 0.45}{\sqrt{0.17\sin\Delta\theta - 3.88\cos\Delta\theta + 25.15}} \right) - 0.04.$$
(18)

To align the planar and spatial linkages the input crank axis of the spatial linkage was placed such that d=-5 and t=0 and the output crank axis such that g=0. Knowing  $d,t,g,\theta_i,\phi_i$  and  $\bar{\gamma}_i$  for  $i=1,\ldots,7$  and solving Eq 13 for (u,v,w,x,y,z) gives the coordinates of  $\mathbf{A}^1$  and  $\mathbf{B}^1$ . The  $\theta_i$  values were adjusted in the range of  $\pm \delta \theta_i$  and the  $\phi_i$  values were adjusted in the range of  $\pm \delta \phi_i$ . The  $\bar{\gamma}_i$  values were recalculated using Eq 18 and the adjusted values of  $\theta_i$ .

Dimensions for Planar Linkage								
GN	ND	DE	EG	$\theta_0$	$k_{0}$			
$r_1$	$r_2$	<i>r</i> <sub>3</sub>	<i>r</i> <sub>4</sub>					
5	0.388	4.994	0.448	-0.045	0.045			

**TABLE 2**. Solution for planar crank rocker for given input parameters

Five hundred variations produced 3582 solutions of which 29 met the design requirements. The 29 design candidates were sorted in ascending order by the link ratio  $\kappa$ , where

$$\kappa = \frac{Longest\ Link\ Length}{Shortest\ Link\ Length} \tag{19}$$

The RMS error of  $\varepsilon$  between each of the top six results and desired pitch function of  $\phi(\theta_k)$  given in Eq 1 was calculated using

$$\varepsilon = \sqrt{\frac{\sum_{k=1}^{n} (\bar{\phi}(\theta_k) - \phi(\theta_k))}{n}},$$
(20)

where  $\bar{\phi}(\theta_k)$  is the pitch function from the solution, and n is the number of samples.

Design number 1 was selected because it has the lowest RMS error of the designs with a link ratio less than 10, see Table 4. Results with link ratios less than 10 improved the ease of manufacturing. Its associated inputs are in Table 3 and the output is plotted in Figure 6.

	Design Input Parameters for Solution 4									
θ	9 0. 0.404 1.173 3.351 5.242 6.087 6.28									
φ	1.571	1.194	0.801	1.83	2.763	1.81	1.571			
γ	0.524	0.653	1.235	2.585	1.185	0.559	0.524			

**TABLE 3**. Table of of randomized input parameters

The mechanism was modeled in SolidWorks see Figure 8 and 9. Figure 7 compares the SolidWorks output, the generated configuration output, and the required pitch angle. The Solid-Works models shows some discrepancy due to minor adjustments to the structure that will allow it to be physically constructed.

#### 9 Conclusion

This paper presents a design methodology for flapping wing mechanisms that control both wing swing and pitch with one input. The resulting mechanism is an RSSR linkage that connects the input and output cranks of a planar four-bar linkage to form spatial sixbar linkage that has a topology similar to the planar Stephenson I. The design procedure is demonstrated for swing and pitch profiles recommended for micro air vehicles. It results in 29 different designs that meet the requirements, one of which is presented in detail.

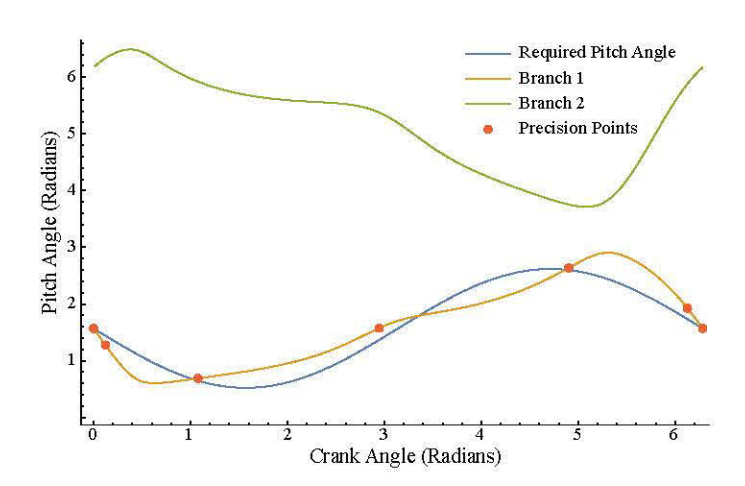
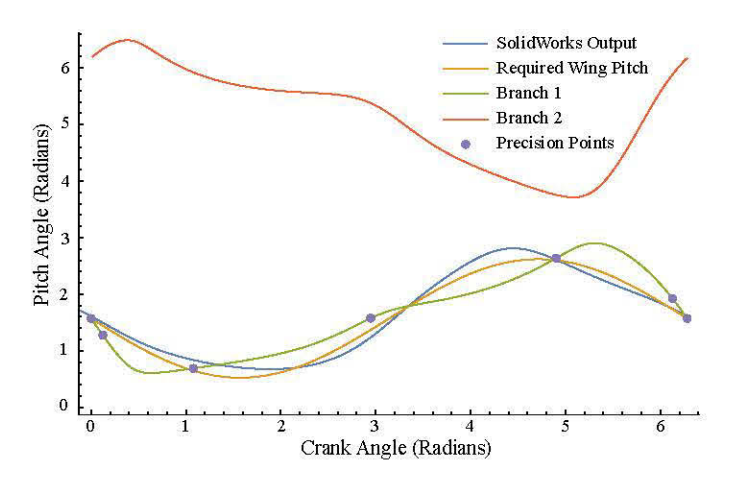
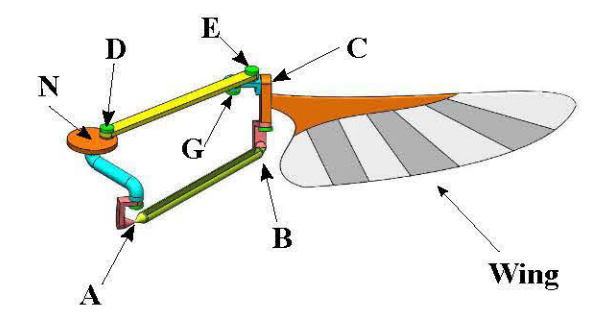


FIGURE 6. The Required Pitch Path vs Selected Pitch Path



**FIGURE 7.** The SolidWorks Pitch Angle vs Required Pitch Path vs Selected Pitch Path



**FIGURE 8**. Isometric View of SolidWorks Model, Ground Link (NG) Not Shown

	Ranked Design Candidates									
			A Coordinates			B Coordinates				
	arepsilon	K	u	v	w	X	y	Z		
1	0.89	2.86	2.25	0.57	-3.32	-1.16	-1.22	1.23		
2	1.39	2.92	7.64	-3.24	-4.31	2.73	0.12	1.67		
3	1.29	3.28	-7.06	-4.66	-4.14	1.21	-2.64	0.22		
4	1.37	3.42	-3.98	-1.87	-4.12	0.72	-1.72	0.47		
5	1.35	12.86	-6.42	-0.52	-5.46	0.15	0.05	-0.64		
6	1.03	16.56	-3.5	-0.02	-4.68	0.01	-0.19	0.31		

**TABLE 4**. Table coordinate solutions

htb	Solution 4 Dimensions for Spatial Linkage									
	NO	OA	AB	BC	CS	SG	$\theta_s$	$\phi_s$		
	$(g_1)$	(a)	(b)	(c)	(s)	(g)				
	-3.98	2.06	6.57	1.44	1.27	0	2.70	3.66		

**TABLE 5**. Table of Link Lengths for the Spatial Mechanism

#### **REFERENCES**

- [1] M. Keennon, K. Klingebiel, H. W., and Andriukov, A., 2012. "Development of the nano hummingbird: A tailless flapping wing micro air vehicle". In AIAA Aerospace Sciences Meeting, AIAA, pp. 1–24.
- [2] Taha, H. E., Nayfeh, A. H., and Hajj, M. R., 2014. "Effect of the aerodynamic-induced parametric excitation on the longitudinal stability of hovering mavs/insects". *Nonlinear Dynamics*, **78**(4), pp. 2399–2408.
- [3] Taha, H. E., Tahmasian, S., Woolsey, C. A., Nayfeh, A. H., and Hajj, M. R., 2015. "The need for higher-order averaging in the stability analysis of hovering mavs/insects". *Bioinspiration and Biomimetics*, 10(1), p. 016002. Selected in the Bioinspiration & Biomimetics Highlights of 2015.
- [4] Svoboda, A., 1948. Computing mechanisms and linkages. McGraw-Hill.
- [5] Freudenstein, F., 1954. "An analytical approach to the design of four-link mechanisms". *Trans. ASME*, 76(3), pp. 483–492.
- [6] Denavit, J., and Hartenberg, R. S., 1960. "Approximate synthesis of spatial linkages". *Journal of Applied Mechan*ics, 27(1), pp. 201–206.
- [7] Suh, C. H., 1968. "Design of space mechanisms for function generation". *Journal of Engineering for Industry*, 90(3), pp. 507–512.
- [8] Gupta, V., 1973. "Kinematic analysis of plane and spatial

# **Top View**

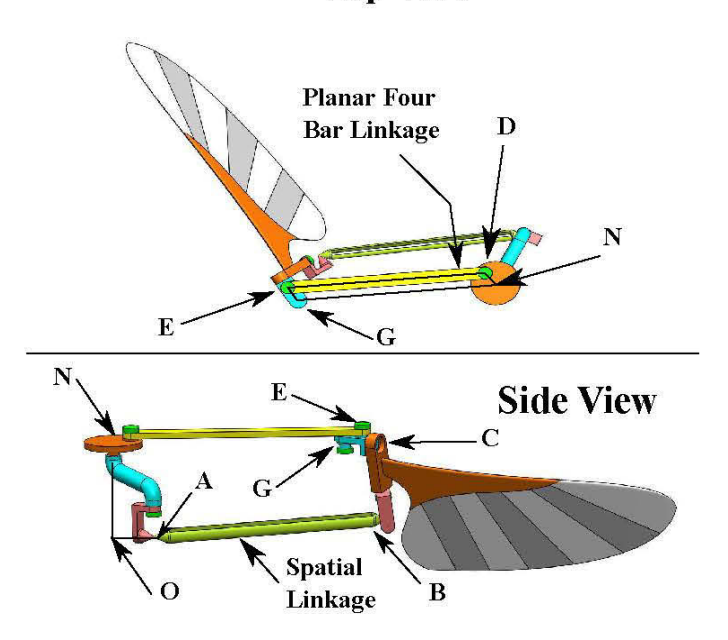


**FIGURE 9.** Top and Side View of SolidWorks Model, Ground Link (NG) Not Shown

- mechanisms". Journal of Engineering for Industry, 95(2), pp. 481–486.
- [9] Dhingra, A., Cheng, J., and Kohli, D., 1994. "Synthesis of six-link, slider-crank and four-link mechanisms for function, path and motion generation using homotopy with m-homogenization". TRANSACTIONS-AMERICAN SOCIETY OF MECHANICAL ENGINEERS JOURNAL OF MECHANICAL DESIGN, 116, pp. 1122–1122.
- [10] Plecnik, M. M., and McCarthy, J. M., 2014. "Numerical synthesis of six-bar linkages for mechanical computation". *Journal of Mechanisms and Robotics*, 6(3), p. 031012.
- [11] Bai, S., Wang, D., and Dong, H., 2016. "A unified formulation for dimensional synthesis of stephenson linkages". *Journal of Mechanisms and Robotics*, 8(4), p. 041009.
- [12] Zhao, P., Purwar, A., and Ge, Q., 2013. "Task driven unified synthesis of planar four-bar and six-bar linkages with revolute and prismatic joints for five position synthesis". In ASME 2013 International Design Engineering Technical Conferences and Computers and Information in Engineering Conference, American Society of Mechanical Engineers, pp. V06AT07A061–V06AT07A061.
- [13] Balta, M., Ahmed, K. A., Wang, P. L., McCarthy, J. M., and Taha, H. E., 2017. "Design and manufacturing of flapping wing mechanisms for micro air vehicles". In 58th AIAA/ASCE/AHS/ASC Structures, Structural Dynamics, and Materials Conference, p. 0509.
- [14] Yan, Z., Taha, H. E., and Hajj, M. R., 2015. "Effects of

- aerodynamic modeling on the optimal wing kinematics for hovering mavs". *Aerospace Science and Technology*, **45**, pp. 39–49.
- [15] Brodell, R. J., and Soni, A., 1970. "Design of the crank-rocker mechanism with unit time ratio". *Journal of Mechanisms*, 5(1), pp. 1–4.
- [16] McCarthy, J. M., and Soh, G. S., 2010. *Geometric design of linkages*, Vol. 11. Springer Science & Business Media.
- [17] Hartenberg, R. S., and Denavit, J., 1964. *Kinematic synthesis of linkages*. McGraw-Hill.
- [18] Innocenti, C., 1995. "Polynomial solution of the spatial burmester problem". *Journal of Mechanical Design*, 117(1), March, pp. 64–68.